ISIJ International, Vol. 40 (2000), No. 2, pp. 161–166

Reactive Casting of Ni–Al–Fe Ternary Intermetallic Alloys

Kiyotaka MATSUURA, Hiroshi JINMON, Yasushi HIRASHIMA,[1)] Tahir I. KHAN[2)] and Masayuki KUDOH

Division of Materials Science and Engineering, Hokkaido University, Sapporo, Hokkaido, 060-8628 Japan.
1) Materials Technology Division, Tokushima Prefectural Industrial Technology Center, Saika, Tokushima, 770-8021 Japan.
2) Department of Materials Engineering, Brunel University, Uxbridge, Middlesex UB8 3PH, UK.

(*Received on September 2, 1999; accepted in final form on November 5, 1999*)

NiAl-base intermetallic alloys containing iron up to 25 at% are produced by reactive casting, which involves an exothermic reaction between elemental liquids and enables one to cast high-melting-point intermetallic alloys without the need of external heating. In this study, aluminum liquid at 1 023 K and a molten nickel-iron alloy at 1 773 K are mixed to produce a molten Ni–Al–Fe ternary intermetallic alloy with a temperature of over 2 300 K, which is approximately 400 K higher than the melting point of the alloy produced. The concentrations of the constituent elements are approximately homogeneous in the ingot of 30 mm in diameter and 130 mm in height. The grain size of the ingot decreases, as the iron content increases. The increase in iron content improves the hardness, bending strength and wear resistance of the alloy. Young's modulus of the alloy decreases with the increase in temperature and iron content.

KEY WORDS: casting; solidification; combustion synthesis; SHS; intermetallic compound; NiAl.

1. Introduction

An intermetallic compound of nickel monoaluminide, NiAl, offers many advantages over conventional superalloys, such as higher melting temperature, lower density, greater specific modulus and higher thermal conductivity.[1)] NiAl also exhibits excellent high-temperature oxidation resistance when doped with zirconium or hafnium, and excellent high-temperature corrosion resistance when doped with chromium or yttrium, that are superior to existing high temperature alloys or coating materials.[1–4)] Therefore, NiAl is a potential low-density and high-strength structural material which might be used at temperatures higher than currently possible with conventional superalloys.

However, when NiAl is produced on an industrial scale by using a conventional casting method, a large amount of energy is consumed because of its high melting point, 1 911 K. It results in a large quantity of fossil fuels consumption and carbon dioxide emission. Energy should be saved from economical and ecological viewpoints.

Recently, the synthesis of NiAl from elemental powders of aluminum and nickel has been studied, by using a self-propagating high-temperature synthesis (SHS) reaction also referred to as reactive sintering.[5–13)] The SHS reaction proceeds exothermically because of a large value of the heat of formation of the reaction product.[14)] Therefore, the SHS reaction provides an energy-saving process for the production of high-melting-point intermetallic compounds such as NiAl.

However, elemental powders usually contain a high level of oxygen, which sometimes reduces the mechanical properties of the product by the SHS. Additionally, metal powder is a high-cost material compared with metal ingots, which leads to a high production cost. We have considered that if elemental liquids are used for the SHS process instead of elemental powders, both the oxygen level in the product and the production cost will be significantly reduced.

The purpose of this study is to investigate (1) the feasibility of the casting of NiAl-base intermetallic alloys by utilizing the exothermic reaction between the elemental liquids and (2) the effect of iron content on the mechanical properties of the alloy.

2. Procedure

Figure 1 shows a schematic drawing of the present method to synthesize NiAl-base intermetallic alloys from the elemental liquids. Molten aluminum at 1 023 K was poured into a porous alumina crucible followed by molten nickel or a nickel-iron alloy at 1 773 K. The two liquids reacted exothermically and then solidified as NiAl or an

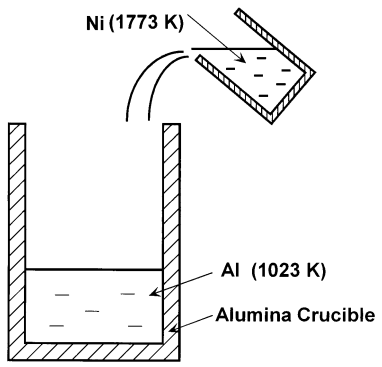

Fig. 1. Schematic drawing showing the reactive casting process.

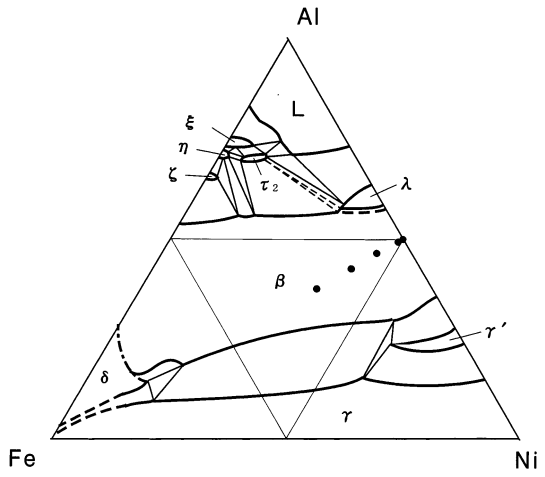

Fig. 2. Compositions of the cast alloys indicated in an Al–Fe–Ni equilibrium ternary phase diagram.[15] Temperature: 1 323 K. Scale: at%.

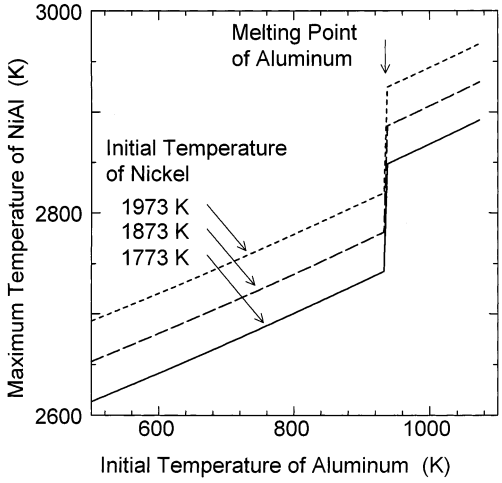

Fig. 3. Calculated maximum temperature of the synthesized NiAl.

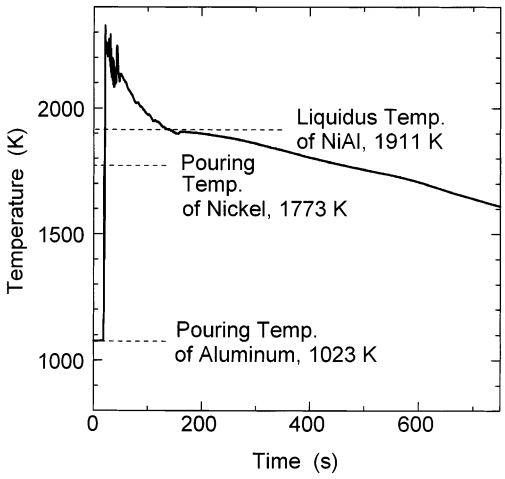

Fig. 4. Change in measured temperature of the mixed liquids.

NiAl-base alloy. The ingot produced was 30 mm in diameter and 130 mm in height. The starting materials were aluminum of 99.99 wt%, nickel of 99.9 wt% and iron of 99.9 wt%. Melting of those elemental metals was carried out in an atmosphere of argon, while pouring in air. The nominal compositions of the cast alloys are indicated on the Al–Fe–Ni equilibrium ternary phase diagram shown in **Fig. 2**.[15] Iron content was varied from 0 to 25 at%, while the molar ratio of nickel and aluminum was fixed at 1 : 1. All the compositions were within the solubility range of the β-phase, (Ni,Fe)Al, which is a fully isomorphous phase from NiAl to FeAl.

The ingot was sectioned for mechanical testing, X-ray diffraction and electron probe microanalyses. Young's modulus was measured at several temperatures from room temperature to 1 473 K in air by using the resonance method. The specimen for the resonance method was approximately 70 mm in length, 15 mm in width and 3 mm in thickness. A Vickers hardness test, a four-point bending test and a pin-on-plate wear test were carried out at room temperature. The applied load for the hardness testing was set at 98 N. The conditions of the bending test were: 3×4 mm^2 in rectangular cross-sectional area of the specimen, 15 mm in distance between the supporting points, 4 mm in distance between the loading points and 0.5 mm/min in cross-head speed. To evaluate the wear resistance of the alloy, the scar depth was monitored during a reciprocal sliding test using a diamond pin under dry conditions, with 1 kg in applied load, 1 Hz in frequency of the reciprocal movement and 5 mm in sliding length. The dynamic change in the coefficient of friction during sliding was also recorded.

3. Results and Discussion

3.1. Heat Generation due to Exothermic Reaction

When the molten nickel was poured into the aluminum liquid, the molten mixture became white hot caused by the heat generation. It results from an exothermic reaction of Ni+Al→NiAl+ΔH_{p298}, where ΔH_{p298} is heat of formation of NiAl at 298 K and is 118 kJ/mol. A simple calculation by using Eqs. (1) through (3) under the adiabatic condition indicates that the maximum temperature of the synthesized NiAl, $T_{MaxNiAl}$, reaches a very high temperature from 2 600 K to 3 000 K, depending on the initial temperatures of aluminum and nickel, as shown in **Fig. 3**.

$$H_{Al}+H_{Ni}+\Delta H_{p298} = \int_{298}^{T_{mNiAl}} C_{NiAl}dT+\Delta H_{NiAl}+\int_{T_{mNiAl}}^{T_{MaxNiAl}} C_{NiAl}dT \quad \text{.....(1)}$$

$$H_{Al}=\int_{298}^{T_{mAl}} C_{Al}dT+\Delta H_{Al}+\int_{T_{mAl}}^{T_{OAl}} C_{Al}dT \quad \text{.....(2)}$$

$$H_{Ni}=\int_{298}^{T_{mNi}} C_{Ni}dT+\Delta H_{Ni}+\int_{T_{mNi}}^{T_{ONI}} C_{Ni}dT \quad \text{.....(3)}$$

where T_0 and T_m are the initial temperature and melting point of the material indicated by the subscript, and C and ΔH are the specific heat and latent heat of the material. This casting technique which involves an exothermic reaction can be used to produce a high-melting-point intermetallic compound without the need of external heating. We therefore named this technique "reactive casting".

Figure 4 shows the change in temperature of the reactive-cast alloy. Temperature was measured on the top sur-

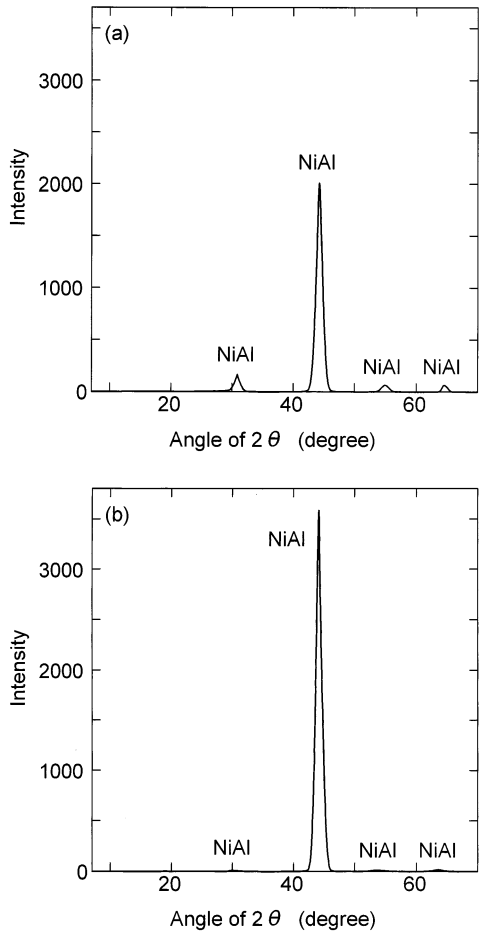

Fig. 5. X-ray diffraction spectra with CuKα radiation. (a) NiAl and (b) NiAl–25at%Fe.

face of the alloy using a spot thermometer. When the aluminum and nickel liquids are mixed, the temperature suddenly goes up to a value over 2 300 K. The measured temperature is lower than that calculated under the adiabatic condition, because heat diffuses from the liquid into the crucible and atmosphere in the practical casting. When the temperature decreases down to the liquidus temperature, a slight stagnation of cooling is observed due to the latent heat of solidification. When molten nickel–iron alloys were poured instead of pure nickel, the temperature of the mixed liquid reached similar temperature values. However, the effect of the iron content on the maximum temperature of the mixed liquid was not clear; the variation in measured temperature was within an experimental error.

3.2. Phase Identification and Chemical Analysis

Figures 5(a) and **5(b)** show the X-ray diffraction spectra of the synthesized NiAl and NiAl–25at%Fe alloy, respectively. In both figures, four peaks were observed; at angles of 30.88, 44.28, 55.00 and 64.05 degree in Fig. 5(a), while 29.96, 44.24, 53.70 and 63.62 degree in Fig. 5(b). These peaks are all very close to those for NiAl with an experimental error range. Figure 5 indicates that the synthesis reaction was completed, because no intermediate reaction product such as Ni_3Al is detected.

When molten Ni–Fe alloys were poured into the molten aluminum to produce the ternary alloys, no additional or external stirring was carried out. We therefore had been

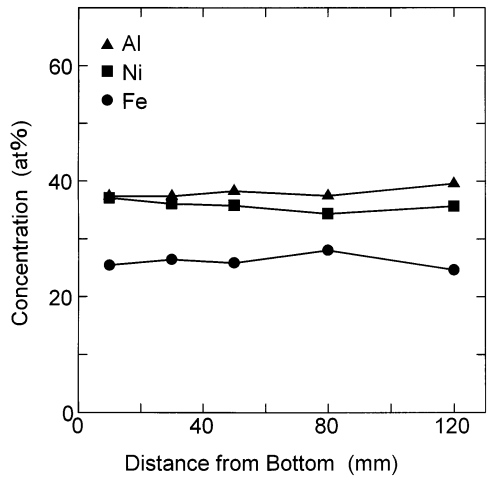

Fig. 6. Concentration profiles of Al, Ni and Fe on a longitudinal section of an NiAl–25at%Fe ingot.

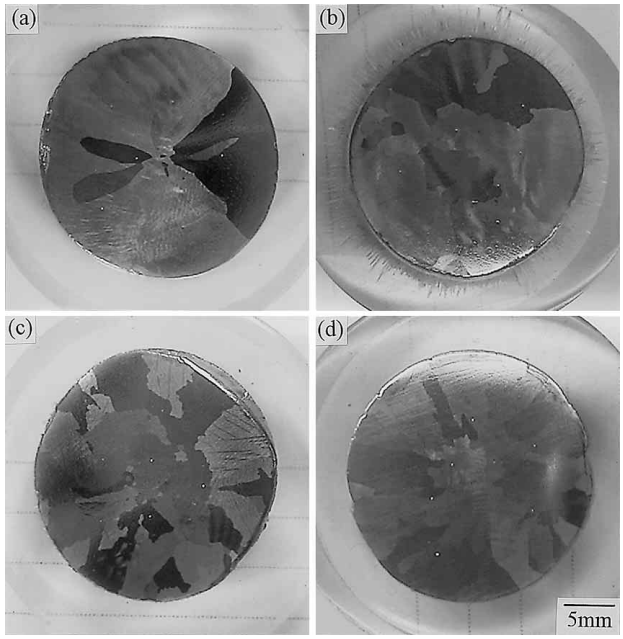

Fig. 7. Grain structure of NiAl–Fe ingots. The iron contents are: (a) 0 at%, (b) 7 at%, (c) 15 at% and (d) 25 at%.

concerned that the mixing of the two liquids might be incomplete. However, the results of the X-ray diffraction testing shown in Fig. 5 indicated that the synthesis reaction was completed. Moreover, **Fig. 6** indicates that the concentrations of the three elements are all approximately constant at the target values over the ingot height. The similar results were also obtained for ingots with other compositions. Therefore, the mixing of the elemental liquids was enough for the complete reaction between them. We consider that the enough mixing was brought about by the convection generated by pouring of the heavier liquid into the lighter liquid and the diffusion at very high temperatures shown in Figs. 3 and 4.

3.3. Metallography

Figure 7 shows the grain structure of the NiAl–Fe ingots. When iron is not added, the ingot has a very large crystal grain size, as shown in Fig. 7(a). The grain size, however, decreases with the increase in iron content (see

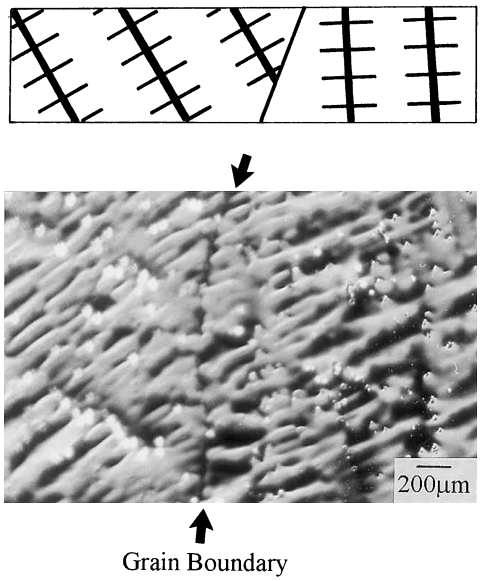

Fig. 8. Microstructure of NiAl, showing dendrite orientations depend on the individual grains.

Figs. 7(b) through 7(d)). It indicates either that the velocity of grain growth decreases, or the number of solidified crystal increases, as the iron content increases. The microstructure of the iron-free NiAl ingot shown in **Fig. 8** supports the latter: the growth direction of the primary dendrite differs depending on the individual grain, which indicates that the grain structure in the ingot was developed not by grain growth but by solidification. Also in all other ingots, individual crystal grains consisted of a colony of dendrites that had a same growth direction. It is likely that a cooling rate after solidification, which is determined to be approximately 0.5 K/s from Fig. 4, is too high for grain growth in NiAl–Fe alloys. The effects of iron on the wettability of the molten alloy to the crucible wall, fragmentation of the growing dendrites and constitutional supercooling of the residual liquid are considered as the possible reasons for the change in grain size.

As the iron content increases, both the concentrations of nickel and aluminum decrease, because the molar ratio of nickel and aluminum was fixed at 1 : 1 in all alloys cast in this study. Because iron is much heavier than aluminum, the increase in iron content increases the density of the alloy, as shown in **Fig. 9**. The density increases from approximately 5.9 to 6.3 Mg/m^3, as the iron content increases from 0 to 25 at%. Those values are much smaller than the density of conventional superalloys, which is approximately 8 Mg/m^3.

3.4. Mechanical Properties

Figure 10 shows the effects of iron content and temperature on the Young's modulus of the alloy. The Young's modulus at room temperature varies from 145 to 172 GPa depending on the iron content, and it decreases with the increase in temperature to 93 to 135 GPa at 1 473 K. In high-iron alloys, generally, the Young's modulus is small, and the decreasing rate of the Young's modulus with the increase in temperature is high, except for the NiAl–1at%Fe alloy. We had suspected an incorrect composition of the alloy, but the results of the analysis indicated that all ingots had the target concentrations of the elements with accuracy within 15%.

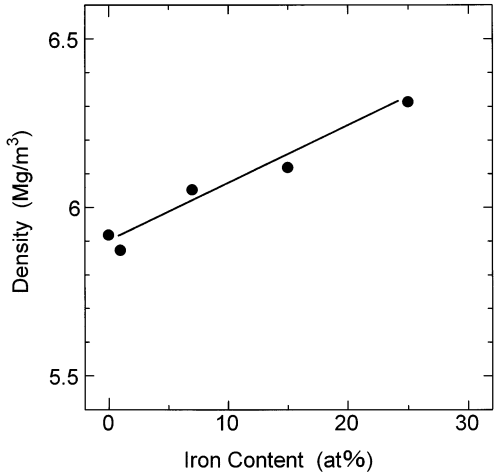

Fig. 9. Effect of iron content on the density of the alloy.

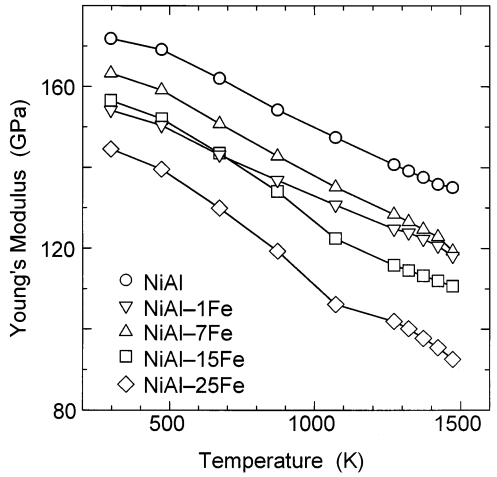

Fig. 10. Effect of iron content on the Young's modulus of the alloy.

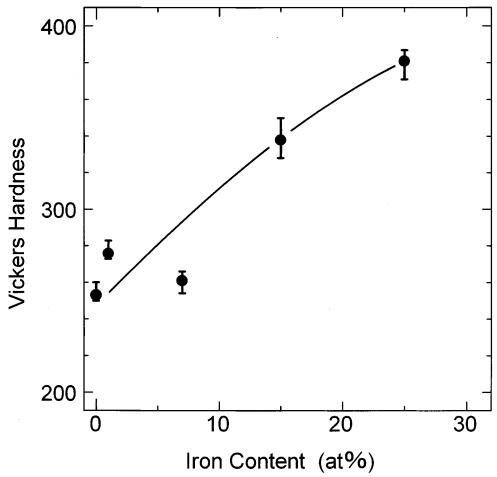

Fig. 11. Effect of iron content on the Vickers hardness of the alloy.

It is not clear yet why the NiAl–1at%Fe alloy shows a deviation in behavior.

Figure 11 shows the effect of iron content on the Vickers hardness of the alloy. The Vickers hardness increases from approximately 260 to 380, as the iron content increases from 0 to 25 at%. The bending strength and wear resistance

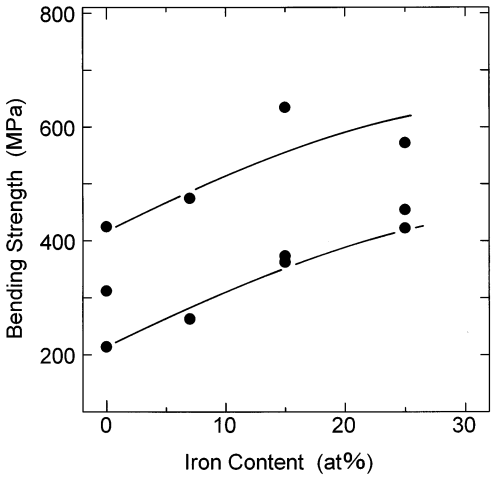

Fig. 12. Effect of iron content on the bending strength of the alloy.

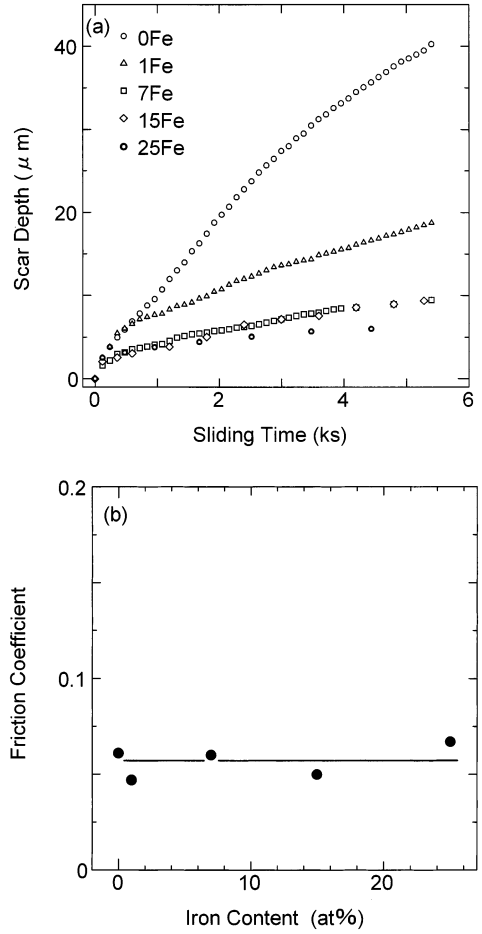

Fig. 13. Effect of iron content on (a) the scar depth and (b) the friction coefficient, measured by sliding of a diamond pin on the alloy plate.

also increase with an increase in iron content, as shown in **Figs. 12** and **13(a)**. It is likely that the increase in hardness, bending strength and wear resistance is due to solution hardening, because the addition of iron to NiAl up to 25 at% does not bring about the precipitation of a new phase such as γ, according to an Al-Fe-Ni equilibrium ternary phase diagram.[15] The friction coefficient measured during the wear test does not change with the iron content, as shown in Fig. 13(b).

We carried out a similar wear test for a low carbon steel, and compared the results with those shown in Fig. 13. The scar depth at a sliding time of 0.5 ks was approximately 85 μm for the low carbon steel, while it was only approximately 5 μm for the NiAl-base intermetallic alloys. The friction coefficient for the low carbon steel was 0.40, while it was only 0.05 for the NiAl-base intermetallic alloys. Those results eloquently tell how excellent wear properties the NiAl-base intermetallic alloys have.

3.5. Assessment of Reactive Casting

We have introduced a new process for casting of intermetallic compounds based on an exothermic reaction between elemental liquids, and have produced Ni–Al–Fe ternary intermetallic alloys. From a viewpoint of the production cost, this process is superior to conventional casting or the SHS process based on an exothermic reaction between elemental powders, as described in Introduction. On the other hand, the properties of the alloy produced by the present process should be compared with those of the alloy produced by the other processes.

Homogeneity in chemical composition in the present ingot is good, as shown in Fig. 6. Young's modulus of approximately 170 GPa at room temperature for the present NiAl, shown in Fig. 10, is close to 188 GPa for an arc-melted NiAl[16]. Vickers hardness of approximately 260 for the present NiAl, shown in Fig. 11, is close to 300 for arc-melted NiAl[17] and is also close to 330 for NiAl produced by the SHS process[12]. Bending strength ranging from 200 to 400 MPa for the present NiAl, shown in Fig. 12, is much higher than that of NiAl produced by the SHS process ranging from 50 to 60 MPa[12] and is comparable to the ultimate tensile strength of induction-melted NiAl of approximately 260 MPa[18]. Consequently, the properties of the NiAl produced by the present process is similar to or better than those of the NiAl produced by the other processes.

4. Conclusions

NiAl-base intermetallic ingots containing iron from 0 to 25 at% were made by reactive casting, which is based on an exothermic reaction between two molten metals. The effects of the iron content on the mechanical properties of the alloy were investigated. The results are summarized as follows:

(1) Aluminum and nickel liquids exothermically react and produce a molten intermetallic compound of NiAl. When the pouring temperatures of aluminum and nickel are 1 023 K and 1 773 K, respectively, the temperature of the NiAl exceeds 2 300 K, which is approximately 400 K higher than the melting point of NiAl. When molten nickel–iron alloys are mixed with molten aluminum, molten NiAl–Fe intermetallic alloys are produced, and the maximum temperature reaches similar values.

(2) The Vickers hardness, bending strength and wear resistance measured at room temperature increase with the increase in iron content of the alloy. The Young's modulus decreases with an increase in both temperature and iron content.

Acknowledgement

The authors gratefully acknowledge the financial support of this work by the Eighth Research Promotion Grant of the Iron and Steel Institute of Japan.

REFERENCES

1) R. D. Noebe, A. Misra and R. Gibala: *ISIJ Int*., **31** (1991), 1172.
2) M. F. Singleton, J. L. Murray and P. Nash: Binary Alloy Phase Diagrams, vol. 1, ed. by T. B. Massalski, ASM, Materials Park, Ohio, (1990), 181.
3) R. Darolia: *J. Met*., **43** (1991), 44.
4) R. L. McCarron, N. R. Lindblad and D. Chatterji: *Corrosion*, **32** (1976), 476.
5) T. Cheng and J. Sun: *Scr. Metall. Mater.*, **30** (1994), 247.
6) T. S. Dyer and Z. A. Munir: *Metall. Mater. Trans. B*, **26B** (1995), 603.
7) M. Inoue and K. Suganuma: *J. Jpn. Inst. Light Metal*, **45** (1995), 209.
8) K. Matsuura, T. Kitamura, M. Kudoh and Y. Itoh: *Mater. Trans. Jpn. Inst. Met*., **37** (1996), 1067.
9) K. Matsuura, T. Kitamura and M. Kudoh: *J. Mater. Process. Tech*., **63** (1997), 298.
10) K. Matsuura, T. Kitamura, M. Kudoh, Y. Itoh and T. Ohmi: *ISIJ Int*., **37** (1997), 87.
11) K. Matsuura and M. Kudoh: *Mater. Sci. Eng*., **A239** (1997), 625.
12) K. Matsuura, K. Ohsasa, N. Sueoka and M. Kudoh: *ISIJ Int*., **38** (1998), 310.
13) K. Matsuura, K. Ohsasa, N. Sueoka and M. Kudoh: *Metall. Mater. Trans. A*, **30A** (1999), 1605.
14) M. Koizumi: Nenshou-Gousei-no Kagaku (Chemistry of Combustion Synthesis), TIC, Osaka, (1992), 31.
15) P. Budberg and A. Prince: Ternary Alloys, vol. 5, ed. by G. Petzow and G. Effenberg, VCH Verlagsgesellschaft , Weinheim, (1993), 309.
16) R. D. Noebe, R. R. Bowman and M. V. Nathal: Physical Metallurgy and Processing of Intermetallic Compounds, ed. By N. S. Stoloff and V. K. Sikka, Chapman and Hall, New York, (1996), 212.
17) V. O. Abramov, S. B. Maslenkov, S. A. Filin and V. S. Russ: *Russ. Metall*., **4** (1989), 161.
18) R. D. Noebe and M. K. Behbehani: *Scr. Metall. Mater*. **27** (1992), 1795.